Preprints of the 21st IFAC World Congress (Virtual)
Berlin, Germany, July 12-17, 2020

Multidimensional Path Tracking With Global Least Squares Solution

Johannes Handler * **Matthew Harker** * **Gerhard Rath** *

* *Chair of Automation, Montanuniversität Leoben, Leoben, Austria (e-mail: {johannes.handler,matthew.harker,gerhard.rath}@unileoben.ac.at).*

Abstract: In this paper, a new method for model based optimal tracking control is presented. The special composition of the cost functional leads to design parameters for constraining the solution so as to ensure that machine limitations are not violated. By minimizing the cost functional with the calculus of variations, or more precisely the Euler-Lagrange equations, the state space representation of the system dynamics is transformed into an augmented state space representation describing the optimal tracking dynamics. The optimal control input is numerically calculated by solving the set of differential equations, given by the augmented state space system, globally with a specialized least-squares solver. The general control approach is demonstrated on an underactuated crane-like system with fixed load hoisting length operating in the horizontal plane. In this case the introduced design parameters determine the trade-off between the cost of tracking accuracy and the cost of using large values of crane speed and acceleration. The potential of the proposed control scheme is proven by both simulation and experimental tests. The multibody simulation is carried out with the software Simscape Multibody^{TM}. For the experimental verification an industrial robot is used whose end effector only moves in a horizontal plane to imitate the trolley of an overhead crane.

Keywords: Trajectory tracking; Overhead crane; Feedforward control; Optimal control; Model-based control;

1. INTRODUCTION

In the last years, the development of autonomous (or self-driving) machines has become a strong research area and one key aspect of self-driving technology is path tracking. The path tracking problem deals with the task of determining speed and steering settings or more generally the control input of a machine in order for a defined point of the machine to follow a certain path. If the desired position is a function of time, it is also referred to as trajectory tracking. One special field where tracking control is used extensively is for cranes where the payload should follow a certain path. In general the load is attached to the trolley with a simple cable, so the load position cannot be directly actuated and in addition the resulting oscillatory behavior can lead to serious difficulties for the human operator. The oscillatory nature of cranes and the fact that they are also underactuated systems makes them a common benchmark problem in control engineering. The general tracking control algorithm proposed in this paper is therefore applied to an overhead crane in order to prove its potential.

Since trajectory tracking is a current topic in many engineering areas several different approaches have been reported in the literature. One idea that is of particular interest to tracking the load of a crane is the suppression of load oscillation. This is because once there are no load oscillations the load position is about the same as the trolley position. For residual oscillation suppression, when performing point to point movements, the most common technique is input shaping (Singhose et al. (1995)). Lately, a modified input shaping method has been developed with the improvement of a zero time delay by Zhao and Tomizuka (2017). Another method that is based on the same idea as input shaping is Delayed Reference Control (DRC) introduced in Boschetti et al. (2014). But unlike input shaping it is feedback control. In order to avoid load sway, oscillation damping is applied by changing the acceleration depending on the measured swing angle while following a predefined path. A crane also fulfills all conditions for a flat system. So, a flat output can be defined in a way, such that the state and input variables can be directly expressed in terms of this flat output. For trajectory tracking this is very useful, because once the trajectory for the flat output is defined, the according trajectories for the states and the input can be deduced immediately, as shown in Fliess et al. (1995) and Böck and Kugi (2014). Feedback Linearization is used for non-linear systems but for this the knowledge of all system states is required, which can be provided by a state observer for all unmeasured states, as shown by Rózsa and Kiss Bálint (2011). For systems with complex kinematics like nonholonomic wheeled mobile robots the most popular method for trajectory tracking is backstepping based control, as proposed in Kumar and Sukavanam (2008) and Sanhoury et al. (2011). An advanced method is stated in Obaid et al. (2016) by implementing constraints and limitations throughout the controller design. For applications where the robustness of the control is of primary importance, it is suggested to use sliding mode control, as in Liu

and Guo (2012). In order to obtain a higher convergence performance, a sliding mode control system based on backstepping is proposed in Wang et al. (2019). The control approach introduced in Le et al. (2013), combines feedback linearization and sliding mode control for trajectory tracking of an overhead crane. Feedback Linearization is used to eliminate the non-linear behavior of the payload swing and sliding mode control is used for cargo lifting and trolley moving. For increasing the robustness of tracking controls various adaptive control methods can be found in the literature. In Ma et al. (2008) an energy-based approach is proposed whereas in Xin et al. (2016) the controller design is done using the finite-time control method. Current research results suggest the use of neural networks (Yang et al. (2020)) as they are particularly suitable for modeling and controlling highly uncertain and nonlinear systems. By using a recurrent neural network for the control system it is possible to learn the behavior of unknown dynamics on-line and adapt accordingly (Yi et al. (2018)). Or they can be used to provide auxiliary inputs for underactuated systems in order to establish the controlability (Liu et al. (2019)). The literature also provides the idea of solving the tracking problem in an optimal sense, to obtain a control that minimizes a defined cost function. In terms of path tracking this cost function often includes the deviation between the actual path and the desired path. In Liu and Jiang (2016) the path tracking problem is transformed into a Bolza problem which is then converted into a nonlinear programming problem by the Gauss pseudospectral method (GPM) and solved with a Sequential Quadratic Programming (SQP) algorithm. Another recently discovered approach is to define the path tracking problem as an LQR problem as shown in Akka and Khaber (2018). Or as suggested in Majd et al. (2018), to also add the deviation of the velocity and the acceleration to the cost function which enables the derivation of an optimal control law from the Hamilton equations. New developments based on model predictive control are presented in Klancar and Skrjanc (2007), Katriniok et al. (2013), Ma and Bao (2018) and Baca et al. (2018).

Since optimal tracking control is crucial for industrial applications in order to increase the productivity of autonomous transportation systems, this paper presents a trajectory tracking approach based on optimal control theory. It is predicated on the work described in Harker and Rath (2018), where a numerical method based on QR decomposition is proposed to solve the tracking problem as an initial value problem. The algorithm in this work solves the tracking problem with the help of the calculus of variations as a boundary value problem and therefore leads to a better result in terms of the residual tracking error.

The contributions of this paper are:

(1) Global Least Squares method to determine the optimal control input for a multidimensional path tracking problem.
(2) A new method to transform the state space representation of the system dynamics into an augmented state space system describing the optimal tracking dynamics where the desired reference trajectory becomes the input of this augmented state space system.
(3) A multibody simulation in Simscape Multibody$^{\text{TM}}$ and experimental tests to verify the proposed control scheme. The test setup consists of a spherical pendulum mounted on an industrial robot. The load position is determined with machine vision tools.

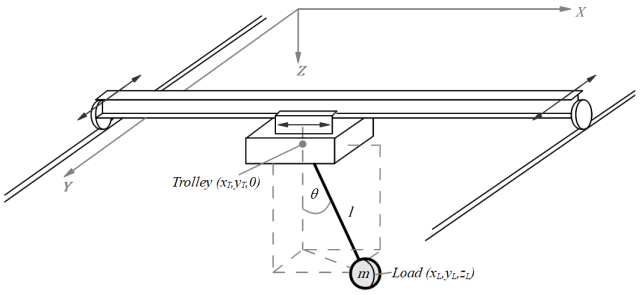

Fig. 1. Diagram of the studied system, a underactuated overhead crane with fixed load hoisting length

2. SYSTEM MODEL

The diagram of an overhead crane on which the tracking control is to be applied is illustrated in Fig. 1. The trolley position is defined by the coordinates (x_T, y_T). The mass m of the load, having the coordinates (x_L, y_L) is accelerated through a cable with a constant length l. We assume that the cable is massless. Since we are only interested in the planar movement of the load the equations of motion have to be derived for the x- and y-direction. Under the assumption that the load sway angle θ is small ($\theta < 10°$) the small-angle approximation,

$$\sin\theta \approx \theta \tag{1}$$

can be used to eliminate the non linearity of the model. This leads to the dynamic equations of the system,

$$\begin{aligned} \ddot{x}_L &= -\tfrac{g}{l}(x_L - x_T) - \tfrac{b}{m}\dot{x}_L \\ \ddot{y}_L &= -\tfrac{g}{l}(y_L - y_T) - \tfrac{b}{m}\dot{y}_L, \end{aligned} \tag{2}$$

where, g is the gravitational constant and b the damping factor, due to friction and drag. The control algorithm is to be verified by a pendulum mounted on an industrial robot. The industrial robot has an integrated position controller for the end effector position and therefore only takes the discretized end effector trajectory as an input value. This leads to a very common two-layer control architecture, where the high-level tracking control determines the required end effector position and speed while the low-level control is in charge of controlling the robot axis in order to reach the set values. Because of this structure the trolley position can be specified as the control input $\boldsymbol{u}$. Hence, $\dot{\boldsymbol{u}}$ and $\ddot{\boldsymbol{u}}$ represent the trolley velocity and acceleration. In order to obtain a state space representation,

$$\dot{\boldsymbol{x}}(t) = \mathsf{A}\boldsymbol{x}(t) + \mathsf{B}\boldsymbol{u}(t), \tag{3}$$

the following states are defined,

$$\begin{aligned} x_1 &= x_L & x_3 &= y_L & u_1 &= x_T \\ x_2 &= \dot{x}_1 & x_4 &= \dot{x}_3 & u_2 &= y_T. \end{aligned} \tag{4}$$

This leads to the final state space representation,

$$\begin{bmatrix} \dot{x}_1 \\ \dot{x}_2 \\ \dot{x}_3 \\ \dot{x}_4 \end{bmatrix} = \begin{bmatrix} 0 & 1 & 0 & 0 \\ -\frac{g}{l} & -\frac{b}{m} & 0 & 0 \\ 0 & 0 & 0 & 1 \\ 0 & 0 & -\frac{g}{l} & -\frac{b}{m} \end{bmatrix} \begin{bmatrix} x_1 \\ x_2 \\ x_3 \\ x_4 \end{bmatrix} + \begin{bmatrix} 0 & 0 \\ \frac{g}{l} & 0 \\ 0 & 0 \\ 0 & \frac{g}{l} \end{bmatrix} \begin{bmatrix} u_1 \\ u_2 \end{bmatrix}. \tag{5}$$

3. CONTROL DESIGN

Since we are dealing with path tracking the criterion to use for minimization, in order to achieve an optimal path, is the path deviation. So, the least-square difference between the actual position $(x_1(t), x_3(t))$ and the desired path $(\xi_x(t), \xi_y(t))$ is a suitable cost function,

$$\int_{t_0}^{t_f} (x_1(t) - \xi_x(t))^2 \, \mathrm{d}t + \int_{t_0}^{t_f} (x_3(t) - \xi_y(t))^2 \, \mathrm{d}t. \quad (6)$$

For the sake of convenience, this can also be written in terms of the state vector by multiplying with the coordinate vectors $\boldsymbol{e}_1$ and $\boldsymbol{e}_3$,

$$\int_{t_0}^{t_f} \left(\boldsymbol{e}_1^{\mathrm{T}}\boldsymbol{x}(t) - \xi_x(t)\right)^2 \, \mathrm{d}t + \int_{t_0}^{t_f} \left(\boldsymbol{e}_3^{\mathrm{T}}\boldsymbol{x}(t) - \xi_y(t)\right)^2 \, \mathrm{d}t. \quad (7)$$

Further, in order to avoid inordinately large control values we should introduce a penalty term. As the control input represents the position, but the speed and acceleration are to be limited, the following regularization term is chosen,

$$\mu_1^2 \int_{t_0}^{t_f} \dot{\boldsymbol{u}}^{\mathrm{T}}(t)\dot{\boldsymbol{u}}(t) \, \mathrm{d}t + \mu_2^2 \int_{t_0}^{t_f} \ddot{\boldsymbol{u}}^{\mathrm{T}}(t)\ddot{\boldsymbol{u}}(t) \, \mathrm{d}t, \quad (8)$$

where the scalar factors μ_1 and μ_2 are called regularization parameters. Note that the introduction of a regularization term is also necessary to obtain a unique solution, according to Kalman (1963). Finally, (5) is included as a constraint via Lagrange multipliers in order to restrict the solution to the system's dynamics. This leads to the functional,

$$\begin{aligned} &J(\boldsymbol{x}(t), \dot{\boldsymbol{x}}(t), \boldsymbol{u}(t), \boldsymbol{\lambda}(t), t) = \\ &\tfrac{1}{2}\int_{t_0}^{t_f} \left(\boldsymbol{e}_1^{\mathrm{T}}\boldsymbol{x}(t) - \xi_x(t)\right)^2 \, \mathrm{d}t + \tfrac{1}{2}\int_{t_0}^{t_f} \left(\boldsymbol{e}_3^{\mathrm{T}}\boldsymbol{x}(t) - \xi_y(t)\right)^2 \, \mathrm{d}t \\ &+\tfrac{\mu_1^2}{2}\int_{t_0}^{t_f} \dot{\boldsymbol{u}}^{\mathrm{T}}(t)\dot{\boldsymbol{u}}(t) \, \mathrm{d}t + \tfrac{\mu_2^2}{2}\int_{t_0}^{t_f} \ddot{\boldsymbol{u}}^{\mathrm{T}}(t)\ddot{\boldsymbol{u}}(t) \, \mathrm{d}t \\ &-\int_{t_0}^{t_f} \boldsymbol{\lambda}^{\mathrm{T}}(t)\left(\dot{\boldsymbol{x}}(t) - \mathsf{A}\boldsymbol{x}(t) - \mathsf{B}\boldsymbol{u}(t)\right) \, \mathrm{d}t. \end{aligned} \quad (9)$$

So the path tracking problem has been transformed into the variational problem of minimizing the functional (9). It can be seen that μ_1 and μ_2 are used to influence the focus of the minimization. If μ_1 and μ_2 are chosen to be large, more focus would be on keeping $\dot{\boldsymbol{u}}$ and $\ddot{\boldsymbol{u}}$ small instead of minimizing the tracking error. In order to perform the tracking as accurately as possible the regularization parameter μ_1 and μ_2 should only be chosen just as large as necessary so that $\dot{\boldsymbol{u}}$ and $\ddot{\boldsymbol{u}}$ do not exceed any machine limitations. We know the start and end values and times because they should be the same as the reference trajectory $(\xi_x(t), \xi_y(t))$, $t \in [t_0, t_f]$, which serve as boundary conditions of the problem. Therefore, we can use the Euler-Lagrange equation to minimize (9), which are, (Courant and Hilbert (1953))

$$\begin{aligned} \tfrac{\partial J}{\partial \boldsymbol{x}} - \tfrac{\mathrm{d}}{\mathrm{d}t}\tfrac{\partial J}{\partial \dot{\boldsymbol{x}}} &= \boldsymbol{0} \\ \tfrac{\partial J}{\partial \boldsymbol{u}} - \tfrac{\mathrm{d}}{\mathrm{d}t}\tfrac{\partial J}{\partial \dot{\boldsymbol{u}}} + \tfrac{\mathrm{d}^2}{\mathrm{d}t^2}\tfrac{\partial J}{\partial \ddot{\boldsymbol{u}}} &= \boldsymbol{0} \\ \tfrac{\partial J}{\partial \boldsymbol{\lambda}} &= \boldsymbol{0}. \end{aligned} \quad (10)$$

Evaluating (10) leads to the system of ordinary differential equations,

$$\begin{aligned} \boldsymbol{e}_1\boldsymbol{e}_1^{\mathrm{T}}\boldsymbol{x} - \boldsymbol{e}_1\xi_x + \boldsymbol{e}_3\boldsymbol{e}_3^{\mathrm{T}}\boldsymbol{x} - \boldsymbol{e}_3\xi_y + \mathsf{A}^{\mathrm{T}}\boldsymbol{\lambda} + \dot{\boldsymbol{\lambda}} &= \boldsymbol{0} \\ \mathsf{B}^{\mathrm{T}}\boldsymbol{\lambda} - \mu_1^2\ddot{\boldsymbol{u}} + \mu_2^2\boldsymbol{u}^{(4)} &= \boldsymbol{0} \\ -\dot{\boldsymbol{x}} + \mathsf{A}\boldsymbol{x} + \mathsf{B}\boldsymbol{u} &= \boldsymbol{0}. \end{aligned} \quad (11)$$

For a system with p states and q controls, this set of equations can be written in the matrix form,

$$\begin{bmatrix} \dot{\boldsymbol{x}} \\ \dot{\boldsymbol{\lambda}} \\ \dot{\boldsymbol{u}} \\ \ddot{\boldsymbol{u}} \\ \boldsymbol{u}^{(3)} \\ \boldsymbol{u}^{(4)} \end{bmatrix} - \begin{bmatrix} \mathsf{A} & 0 & \mathsf{B} & 0 & 0 & 0 \\ -\mathsf{E}_{13} & -\mathsf{A}^{\mathrm{T}} & 0 & 0 & 0 & 0 \\ 0 & 0 & 0 & \mathsf{I}_q & 0 & 0 \\ 0 & 0 & 0 & 0 & \mathsf{I}_q & 0 \\ 0 & 0 & 0 & 0 & 0 & \mathsf{I}_q \\ 0 & -\frac{1}{\mu_2^2}\mathsf{B}^{\mathrm{T}} & 0 & 0 & \frac{\mu_1^2}{\mu_2^2}\mathsf{I}_q & 0 \end{bmatrix} \begin{bmatrix} \boldsymbol{x} \\ \boldsymbol{\lambda} \\ \boldsymbol{u} \\ \dot{\boldsymbol{u}} \\ \ddot{\boldsymbol{u}} \\ \boldsymbol{u}^{(3)} \end{bmatrix} - \begin{bmatrix} \boldsymbol{0} & \boldsymbol{0} \\ \boldsymbol{e}_1 & \boldsymbol{e}_3 \\ \boldsymbol{0} & \boldsymbol{0} \\ \boldsymbol{0} & \boldsymbol{0} \\ \boldsymbol{0} & \boldsymbol{0} \\ \boldsymbol{0} & \boldsymbol{0} \end{bmatrix} \begin{bmatrix} \xi_x \\ \xi_y \end{bmatrix} = \boldsymbol{0} \quad (12)$$

with

$$\mathsf{E}_{13} = \boldsymbol{e}_1\boldsymbol{e}_1^{\mathrm{T}} + \boldsymbol{e}_3\boldsymbol{e}_3^{\mathrm{T}}. \quad (13)$$

By defining,

$$\boldsymbol{\gamma} = \left[\boldsymbol{x} \ \boldsymbol{\lambda} \ \boldsymbol{u} \ \dot{\boldsymbol{u}} \ \ddot{\boldsymbol{u}} \ \boldsymbol{u}^{(3)}\right]^{\mathrm{T}}, \quad (14)$$

we can write (12) compactly as,

$$\dot{\boldsymbol{\gamma}} - \mathsf{M}\boldsymbol{\gamma} - \mathsf{N}\boldsymbol{\xi} = \boldsymbol{0}. \quad (15)$$

Note, that this system of differential equations is of the same form as (3) and therefore can be seen as an augmented state space representation of the optimal tracking movement where the given reference trajectory $\boldsymbol{\xi}$ has become the control input. Now, solving this system of differential equations for $\boldsymbol{\gamma}$ provides the sought after control input $\boldsymbol{u}$ of the original system. However, this set of equations expresses a continuous system. But the control input should be determined for a given reference trajectory $(\xi_x(n), \xi_y(n))$ defined in discrete time steps $n \in [n_0, n_f]$, since standard PLCs work in a discrete domain. Therefore, the system (15) has to be discretized over this interval. The individual states of $\boldsymbol{\gamma}$ can be discretized directly as a vector,

$$\boldsymbol{\gamma}_k = \begin{bmatrix} \gamma_k(t_0) \\ \gamma_k(t_1) \\ \vdots \\ \gamma_k(t_f) \end{bmatrix}. \quad (16)$$

With this representation the state vector becomes, for a system with p states discretized into n evenly spaced time steps, a vector of p stacked vectors with altogether np elements,

$$\boldsymbol{\gamma} = \begin{bmatrix} \boldsymbol{\gamma}_1 \\ \boldsymbol{\gamma}_2 \\ \vdots \\ \boldsymbol{\gamma}_p \end{bmatrix}. \quad (17)$$

Further, the derivative of one state can simply be calculated by the multiplication with a suitable numerical differentiation matrix D (see Harker (2020)),

$$\dot{\boldsymbol{\gamma}}_k \approx \mathsf{D}\boldsymbol{\gamma}_k. \quad (18)$$

Since this computation has to be done for each state the differentiation matrix can be combined with a $p \times p$ identity

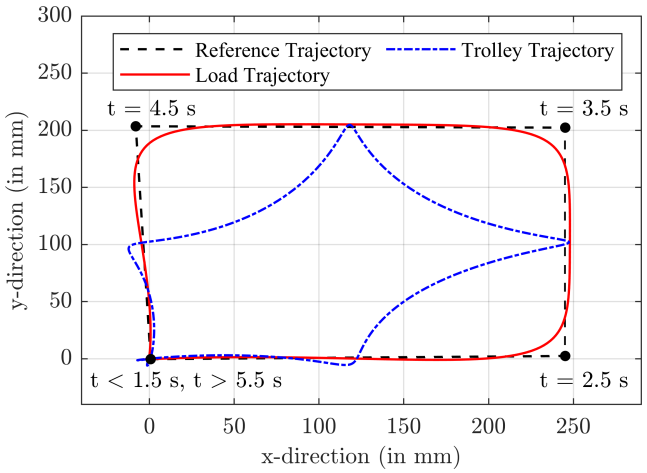

Fig. 2. Optimal control for a desired trajectory and estimation for the actual load trajectory

matrix by the Kronecker product and then applied to the whole state vector,

$$\dot{\boldsymbol{\gamma}} \approx (\mathsf{I}_p \otimes \mathsf{D})\boldsymbol{\gamma}. \tag{19}$$

This also has to be done with the matrices M and N which leads to the final representation,

$$(\mathsf{I}_p \otimes \mathsf{D})\boldsymbol{\gamma} = (\mathsf{M} \otimes \mathsf{I}_n)\boldsymbol{\gamma} + (\mathsf{N} \otimes \mathsf{I}_n)\boldsymbol{\xi}. \tag{20}$$

Rearranging this equation yields the final formulation,

$$\mathsf{L}\boldsymbol{\gamma} - \boldsymbol{f} = \mathbf{0}. \tag{21}$$

with,

$$\begin{aligned} \mathsf{L} &= \mathsf{I}_p \otimes \mathsf{D} - \mathsf{M} \otimes \mathsf{I}_n \\ \boldsymbol{f} &= (\mathsf{N} \otimes \mathsf{I}_n)\boldsymbol{\xi}. \end{aligned} \tag{22}$$

Equation (21) can be solved with a least-squares solver for the state vector $\boldsymbol{\gamma}$. In this work the MATLAB solver *lsqlin()*, which is a linear least-squares solver with equality constraints, is used to solve this task, in order to incorporate the boundary conditions. For a rest-to-rest movement the boundary conditions can be designated as,

$$\begin{array}{lll} \gamma_1(t_0) = \xi_x(t_0) & \gamma_3(t_0) = \xi_y(t_0) & \gamma_9(t_0) = \xi_x(t_0) \\ \gamma_1(t_f) = \xi_x(t_f) & \gamma_3(t_f) = \xi_y(t_f) & \gamma_9(t_f) = \xi_x(t_f) \\ \gamma_2(t_0) = 0 & \gamma_4(t_0) = 0 & \gamma_{10}(t_0) = \xi_y(t_0) \\ \gamma_2(t_f) = 0 & \gamma_4(t_f) = 0 & \gamma_{10}(t_f) = \xi_y(t_f) \\ \gamma_{11}(t_0) = 0 & \gamma_{12}(t_0) = 0 & \gamma_{13}(t_0) = 0 \\ \gamma_{11}(t_f) = 0 & \gamma_{12}(t_f) = 0 & \gamma_{13}(t_f) = 0 \\ \gamma_{14}(t_0) = 0 & \gamma_{14}(t_f) = 0 & \end{array} \tag{23}$$

With the assignments made in (4) and (14) these conditions represent physical values. They ensure, that the position of the load and the trolley meet the reference path $\boldsymbol{\xi}$ at the start and at the end. Since we are talking about a rest-to-rest movement the velocity of both, the load and the trolley, has to be zero at the beginning as well as at the end. Solving (21) and (23) for $\boldsymbol{\gamma}$ as a least-squares with equality constraints problem not only delivers the optimal control input $\boldsymbol{u}$, but also gives us an estimation for the load trajectory $(\gamma_1(t), \gamma_3(t))$ based on the dynamics (5). For a miniature system of an overhead crane, which is also used for the laboratory verification, with the parameters shown in Table 1, the solution and the estimated load trajectory can be seen in Fig. 2. As reference trajectory a slightly skewed rectangular path is chosen. It has to be mentioned that the reference trajectory is designed to remain at the initial and final position for 1.5 s to achieve smoother

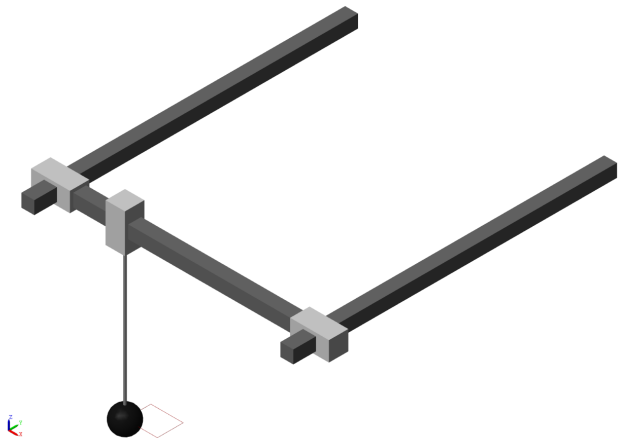

Fig. 3. Multibody model used for the simulation

results and is defined for the time interval $t \in [0, 7]$s. Along the long edges and the short edges the load should respectively travel with a constant speed of 0.25 m/s and 0.2 m/s. The reference trajectory $\boldsymbol{\xi}$ is discretized with 10 ms time steps.

4. VERIFICATION

4.1 Multibody Simulation

The results of the proposed optimal path tracking algorithm for an overhead crane are first confirmed by a multibody simulation. For the simulation the software Simscape Multibody$^{\text{TM}}$ is used and the simulation parameters are the same as for the calculation of the optimal control input $\boldsymbol{u}$, shown in Table 1. See Fig. 3 for the multibody model used for the simulation. The load suspension is modeled by a spherical joint to provide three rotational degrees of freedom i.e., a spherical pendulum. The motion in the horizontal plane is obtained by two actuated prismatic joints. The simulated path is shown in Fig. 4. Furthermore, it can be seen in Fig. 4, that the state space model (5) describes the dynamics of the system quite well and that for the chosen reference trajectory the small angle approximation (1) is a permissible method to linearize the system model.

4.2 Experimental Tests

For the experimental validation an industrial robot was used to imitate an overhead crane, shown in Fig 5. The end effector of the robot only moves in a horizontal plane and is therefore a proper representation of the trolley. The load is equipped with a laser-pointer on the bottom pointing down. This laser-pointer is used to determine the load position because it can be said that the marked position on the floor is equal to the load position. It has

Table 1. Model parameters

Parameter	Value
l (in m)	1.316
m (in kg)	0.419
b (in kg/s)	0
μ_1	$0.5 \cdot 10^{-3}$
μ_2	$0.5 \cdot 10^{-3}$

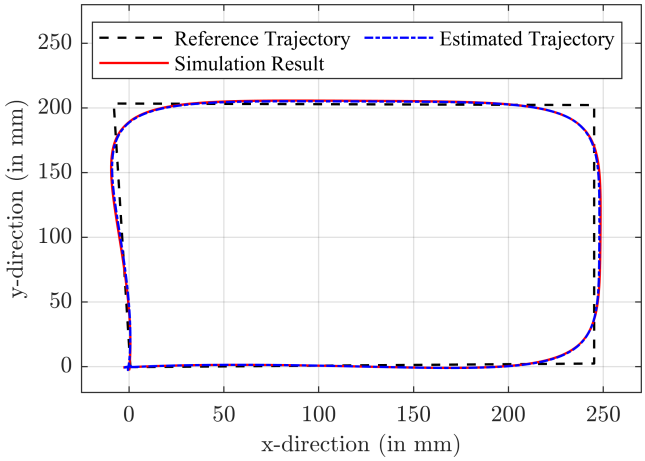

Fig. 4. Comparison of the simulation result and the expected load trajectory

Fig. 5. Experimental setup used for the validation of the proposed method

to be mentioned, due to the pendulum tilt there occurs a small deviation between the actual pendulum position and the marked position on the floor because the laser beam always points in the direction of the load suspension and not exactly in the vertical direction. Therefore, the length of the load suspension is chosen in a way such that there is only a small gap ($\sim$ 10 mm) between the load and the floor, in order to keep this error as small as possible. According to the simulation the largest pendulum tilt is about 4° which leads to a maximum deviation in the order of 10^{-3} m. During the execution of the control algorithm the laser dot on the floor is filmed. Afterwards the video is evaluated frame by frame with machine vision tools

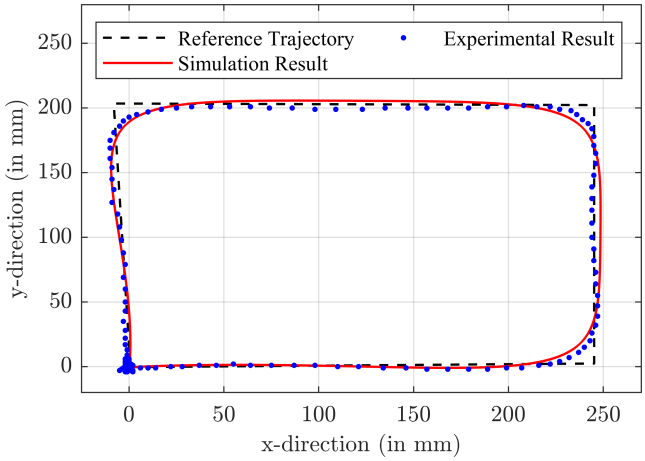

Fig. 6. Result of the simulation and the experimental test displayed in the horizontal plane

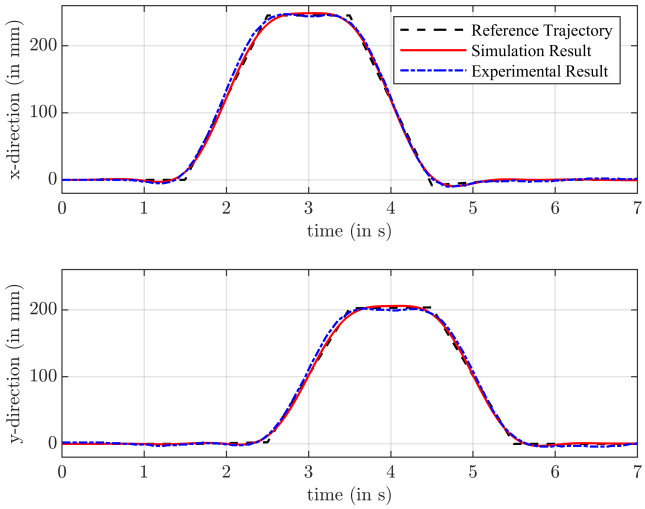

Fig. 7. Result of the simulation and the experimental test as a function of time

to obtain the load position for each frame, whereby the payload trajectory can be established. The results of the simulation as well as the experimental results are shown in Fig. 6 and Fig. 7. The outcome of the experimental tests shows that the reference trajectory is tracked with good accuracy. The slight difference between the simulation result and the measurement result can be explained by the fact that the damping coefficient b was set to zero for the simulation which does not exactly reflect reality.

5. CONCLUSION

This paper proposed a new model based optimal tracking control approach with the application to an overhead crane. The tracking problem was transformed into a variational problem with known initial and final values. With the Euler-Lagrange equations an augmented state space system describing the optimal tracking movement was obtained, where the desired reference trajectory has become the control input. Thereby, two design parameters μ_1 and μ_2 have been introduced. For the case of the overhead crane they are used to ensure that the resulting control input does not exceed any machine limitations, so that the results can be applied to real world systems. The desired

control input was calculated by solving the augmented state space system with a least-squares method for the whole path at once. This gives you the advantage of a global optimal solution in a least-squares sense. Another advantage of the proposed control scheme is its ease of implementation as it can simply be put ahead of an already existing machine position controller. The potential of the proposed control scheme has been proven by experimental and simulation results.

ACKNOWLEDGEMENTS

This project was inspired by the *EIT RawMaterials* project *Rock Vader*.

REFERENCES

Akka, K. and Khaber, F. (2018). Optimal tracking control of a trajectory planned via fuzzy reactive approach for an autonomous mobile robot. *International Journal of Advanced Robotic Systems*.

Baca, T., Hert, D., Loianno Giuseppe, Saska, M., and Kumar, V. (2018). Model predictive trajectory tracking and collision avoidance for reliable outdoor deployment of unmanned aerial vehicles. In *2018 IEEE/RSJ International Conference on Intelligent Robots and Systems*.

Böck, M. and Kugi, A. (2014). Manifold stabilization and path-following control for flat systems with application to a laboratory tower crane. In *53rd IEEE Conference on Decision and Control*, 4529–4535.

Boschetti, G., Caracciolo, R., Richiedei, D., and Trevisani, A. (2014). A non-time based controller for load swing damping and path-tracking in robotic cranes. *Journal of Intelligent & Robotic Systems*, 76(2), 201–217.

Courant, R. and Hilbert, D. (1953). *Methods of Mathematical Physics*. Interscience Publishers, Inc, New York.

Fliess, M., Lévine, J., Martin, P., and Rouchon, P. (1995). Flatness and defect of nonlinear systems: Introductory theory and examples. *International Journal of Control*, 61, 1327–1361.

Harker, M. (2020). *Fractional Differential Equations: Numerical Methods for Applications*. Springer International Publishing, 1 edition.

Harker, M. and Rath, G. (2018). Discrete inverse problem approach to path tracking in state space form. In *23rd International Conference on Applied Electronics*, 41–44.

Kalman, R.E. (1963). The theory of optimal control and the calculus of variations. In R. Bellmann (ed.), *Mathematical Optimization Techniques*, 309–331. University of California Press, Berkeley.

Katriniok, A., Maschuw, J.P., Christen, F., Eckstein, L., and Abel, D. (2013). Optimal vehicle dynamics control for combined longitudinal and lateral autonomous vehicle guidance. In *2013 European Control Conference (ECC)*. IEEE.

Klancar, G. and Skrjanc, I. (2007). Tracking-error model-based predictive control for mobile robots in real time. *Robotics and Autonomous Systems*, 55, 460–469.

Kumar, U. and Sukavanam, N. (2008). Backstepping based trajectory tracking control of a four wheeled mobile robot. *International Journal of Advanced Robotic Systems*, 5(4), 403–410.

Le, T.A., Lee, S.G., and Moon, S.C. (2013). Partial feedback linearization and sliding mode techniques for 2d crane control. *Transactions of the Institute of Measurement and Control*, 36, 78–87.

Liu, D. and Guo, W. (2012). Tracking control for an underactuated two-dimensional overhead crane. *Journal of Applied Research and Technology*, 10, 597–606.

Liu, P., Yu, H., and Cang, S. (2019). Adaptive neural network tracking control for underactuated systems with matched and mismatched disturbances. *Nonlinear Dynamics*.

Liu, Y. and Jiang, J. (2016). Optimum path-tracking control for inverse problem of vehicle handling dynamics. *Journal of Mechanical Science and Technology*, 30, 3433–3440.

Ma, B., Fang, Y., and Zhang, X. (2008). Adaptive tracking control for an overhead crane system. In *17th IFAC World Congress*, 12194–12199.

Ma, X. and Bao, H. (2018). An anti-swing closed-loop control strategy for overhead cranes. *Applied Science*, 8, 1463–1474.

Majd, K., Razeghi-Jahromi, M., and Homaifar, A. (2018). Optimal kinematic-based trajectory planning and tracking control of autonomous ground vehicle using the variational approach. In *IEEE Intelligent Vehicles Symposium (IV)*, 585–590.

Obaid, M.A.M., Husain, A.R., and Al-kubati, A.A.M. (2016). Robust backstepping tracking control of mobile robot based on nonlinear disturbance observer. *International Journal of Electrical and Computer Engineering*, 6(2), 901–908.

Rózsa, T. and Kiss Bálint (2011). Tracking control for two-dimensional overhead crane: Feedback linearization with linear observer. In *ICINCO*.

Sanhoury, I.M., Amin, S.H., and Husain, A.R. (2011). Trajectory tracking of steering system mobile robot. In *4th International Conference on Mechatronics (ICOM)*.

Singhose, W., Singer, N., and Seering, W. (1995). Comparison of command shaping methods for reducing residual vibration. In *3rd European Control Conference*, 1126–1131.

Wang, P., Gao, S., Li, L., Cheng, S., and Zhao, L. (2019). Automatic steering control strategy for unmanned vehicles based on robust backstepping sliding mode control theory. *IEEE Access*, 7.

Xin, L., Wang, Q., and She, Jinshua, Li Yuan (2016). Robust adaptive tracking control of wheeled mobile robots. *Robotics and Autonomous Systems*, 78, 36–48.

Yang, T., Sun, N., Chen, H., and Fang, Y. (2020). Neural network-based adaptive antiswing control of an underactuated ship-mounted crane with roll motions and input dead zones. *IEEE Transactions on Neural Networks and Learning Systems*, 31(3), 901–914. doi: 10.1109/TNNLS.2019.2910580.

Yi, G., Mao, J., Wang, Y., Guo, S., and Miao, Z. (2018). Adaptive tracking control of nonholonomic mobile manipulators using recurrent neural networks. *International Journal of Control, Automation and Systems*, 16, 1390–1403.

Zhao, Y. and Tomizuka, M. (2017). Modified zero time delay input shaping for industrial robot with flexibility. In *ASME 2017 Dynamic Systems and Control Conference*.